The contribution of Sahara dust to ice nucleating particle concentrations at the High Altitude Station Jungfraujoch (3580 m a.s.l.), Switzerland

Cyril Brunner[1], Jie Chen[1], Benjamin T. Brem[2], Martine Collaud Coen[3], Franz Conen[4], Maxime Hervo[3], Stephan Henne[5], Martin Steinbacher[5], Martin Gysel-Beer[2], and Zamin A. Kanji[1*]

1Institute for Atmospheric and Climate Science, ETH, Zurich, CH-8092, Switzerland
2Laboratory of Atmospheric Chemistry, Paul Scherrer Institute, CH-5232 Villigen PSI, Switzerland
3Federal Office of Meteorology and Climatology, MeteoSwiss, CH-1530 Payerne, Switzerland
4Department of Environmental Sciences, University of Basel, CH-4056 Basel, Switzerland
5Laboratory for Air Pollution/Environmental Technology, Empa, CH-8600 Dübendorf, Switzerland

Contact: zamin.kanji@env.ethz.ch and jie.chen@env.ethz.ch

1 Introduction and Motivation

- Aerosol-ice cloud interactions are highly uncertain because the abundance, physicochemical natures and sources of ice nucleating particles (INPs) remain largely unconstrained. Mineral dust has been found to be the most abundant INP species in the atmosphere, however, the contribution of mineral dust to the total INP population remains unknown.

-The limitations of the available autonomous online instruments impede our understanding on the spatiotemporal variability and the evolution of INPs in the atmosphere.

The goals of this work:

(1) To develop a fully automated counter and implement the online monitoring of INPs at one of the GAW station (Jungfraujoch, JFJ)

(2) To investigate the frequency of Sarah dust events and their contribution to atmospheric INPs at JFJ based on the targeted field campaigns

2 Development of HINC-Auto

The Automated Horizontal Ice Nucleation Chamber (HINC-Auto)

- **Thermal Gradient Diffusion principle**
- **A schematic of HINC-Auto**

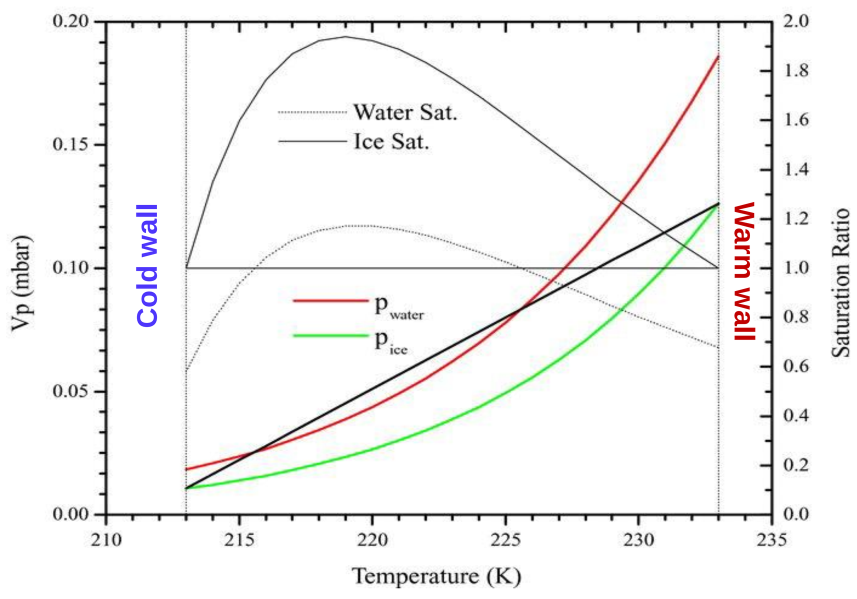

Kanji and Abbatt et al., (2009), Aerosol. Sci. Tech.

Figure 1. Supersaturation profile in the continuous flow diffusion chamber (CFDC), here represented by UT-CFDC

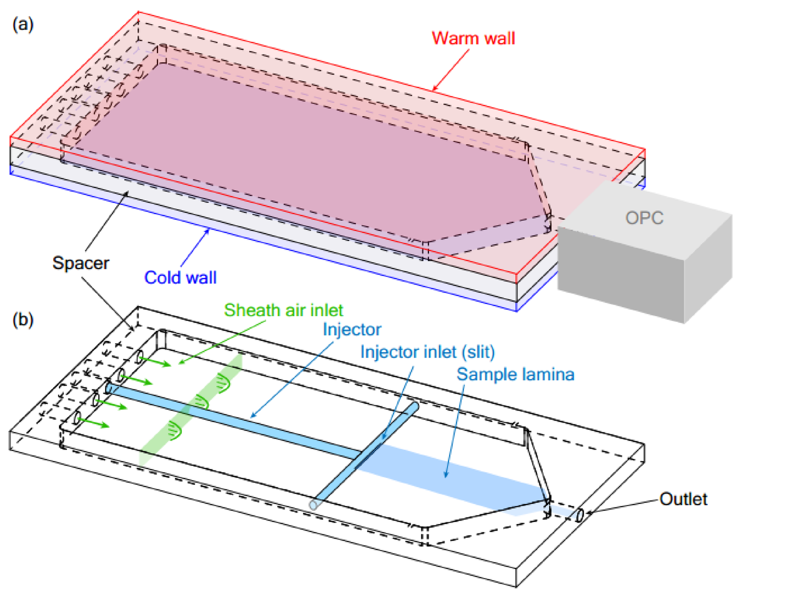

Brunner and Kanji et al., (2021), Atmos. Meas. Tech

Figure 2. A schematic of HINC, the building platform of HINC-Auto: (a) the entire chamber, and (b) the internal parts.

- **Improvements and validations of HINC-Auto**

Hardware Designs

Ideal flow field within chamber

- A mesh was introduced to smooth the sheath air

Longer sampling time, Lower economic cost

- Machining the walls in aluminum
- Reduction of the chamber length
- Pre-cooling of the sheath air

Software development

Automated/Remote control, Online data processing

- A newly developed Python-based guided user interface

Validations

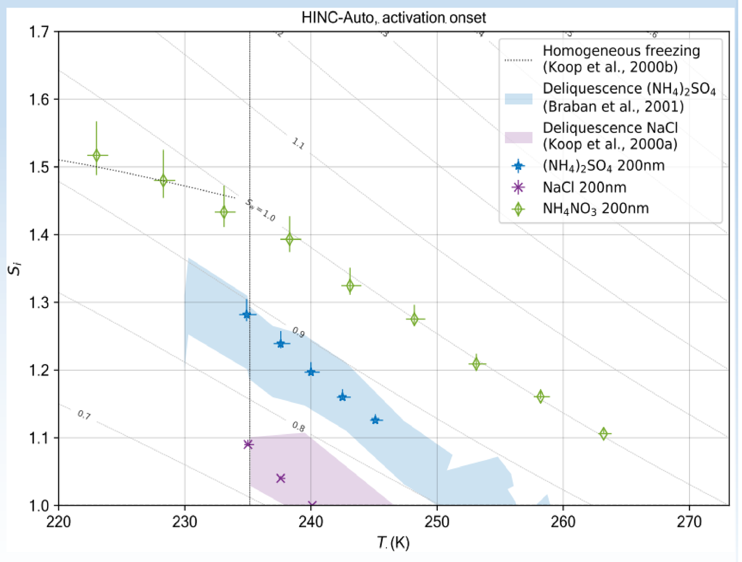

Brunner and Kanji et al., (2021), Atmos. Meas. Tech

Figure 3. Data from experiments in HINC-Auto and values from literature for deliquescence, cloud droplet formation, and homogeneous freezing onset with standard substances.

3 Deployment of HINC-Auto for the field campaign

The Jungfraujoch (JFJ) field compagin

- **JFJ Site description:** a mountain top station

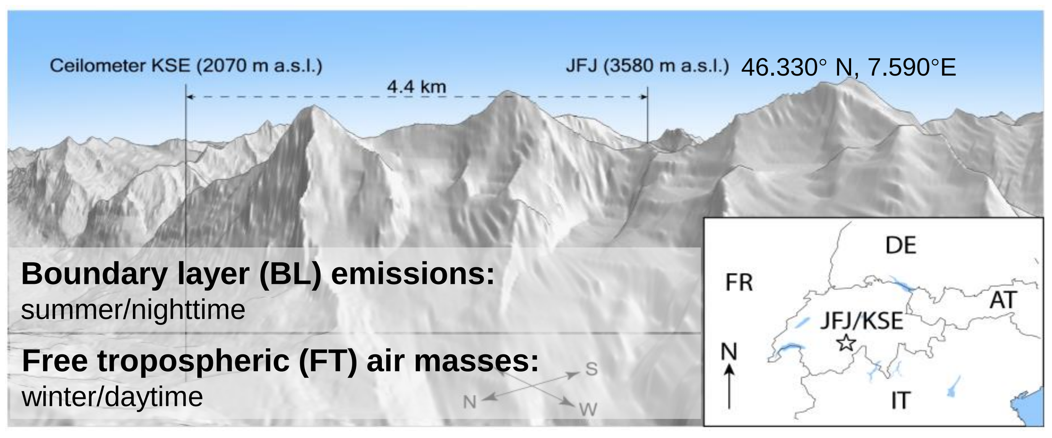

Figure 4. Illustration of the location of the INP sampling location at the JFJ within the topography and in Switzerland. The topography was extracted from the digital height model DHM25 from the *Federal Office of Topography swisstopo*.

- **INP measurements:**

- Time periods: Feb. 7, 2020 – Jan. 31, 2021
- Mixed-phase cloud relevant conditions: T= 243.15 K and S_w= 1.04
- The longest continuous INP datasets recorded with online INP instrument

- **Other measured parameters**

Aerosols and Gases

- Trace gases (CO, NOy) (EMPA)
- Aerosol plume retrieval (ceilometer, MeteoSwiss)
- PM chemical composition (EMPA)
- Aerosol number size distributions (PSI)
- Light scattering/absorption coefficient (PSI)

Cloud Microphysics

- CCN number concentration (PSI)

Models and other techniques

- Primary ice formation (COSMO model, ETH)
- FLEXPART particle residence time (EMPA)
- Dust retrieved from satellite remote sensing (CAMS)

Acknowledgements

This work is supported by the following projects: MeteoSwiss GAW-CH (2018~2021)

4 Results

4.1 Classification of Sahara dust event (SDE) and air masses

- **Four tracers for SDE**

Albedo Ångström exponent Y: Negative more than 6h	Attenuated backscatter Y: aerosol plume 3200-4000 m a.s.l
Particle surface residence times Y: >1000 s m³ kg	Satellite-retrieved dust mass concentrations Y: $dust_{CAM}$>2.36 μg/m³

1. Number of Y=0, background period (BG)
2. Number of 1≤Y < 4, low confidence SDE (lcSDE)
3. Number of Y=4, high confidence SDE (hcSDE)

- **Indicators for air masses from BL**

222-Radon concentration

$$PDF_{FT}(^{222}Rn) = \frac{1}{\sigma_{FT}\sqrt{2\pi}} e^{-\frac{1}{2}\left(\frac{\log_{10}(222Rn)-\mu_{FT}}{\sigma_{FT}}\right)^2} \quad (Eq.1)$$

Concentration of particles larger than 90 nm (N_{90})

The probability of the sampled air in FT origin

$$P_{FT} = \frac{PDF_{FT}(^{222}Rn)}{PDF_{FT}(^{222}Rn)+PDF_{BL}(^{222}Rn)} \frac{1}{1+e^{k(N_{90}-N_{90,TH})}} \quad (Eq.2)$$

1. P_{FT}≥50%, JFJ within FT air masses
2. P_{FT}<50%, JFJ within BL air masses

SDEs occur in FT (FT_{SDE}) | **SDEs occur in BL (BL_{SDE})**

Non SDE, Background period (BG)

26 SDEs were detected and identified (14 hcSEDs, 12 lcSEDs; 14% of the spanned time)

4.2 Dust significantly contribute to INPs at 243 K at the JFJ

- **SDEs increased INP concentrations**

hcSDE (28.5 std L^{-1})>lcSDE (13.1 std L^{-1})>non-SDE (1.1 std L^{-1})

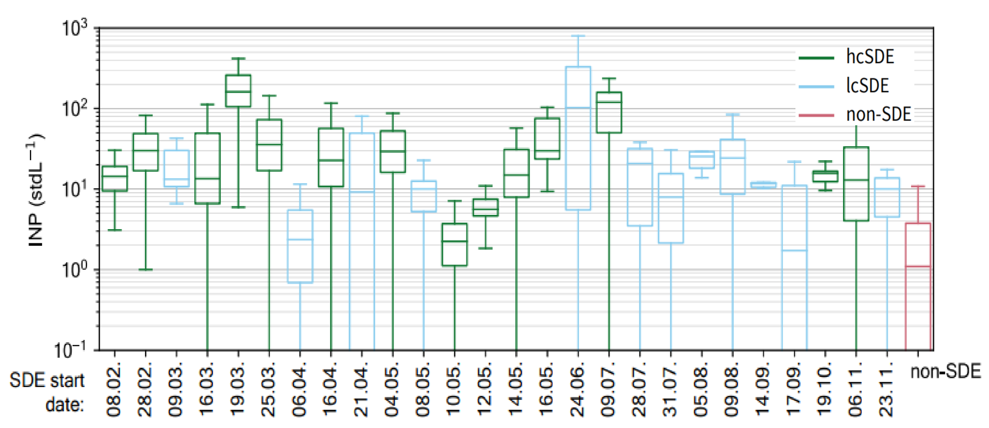

Figure 5. plots from all 26 SDEs, color-coded as 14 high confidence SDEs (hcSDE) or 12 low confidence SDEs (lcSDE), respectively, and the non-SDE periods: median with 25th to 75th percentiles, whiskers: 5th to 95th percentiles.

- **Dust contributes 97.7% of INPs**

Dust INP contribution during SEDs:

$$\frac{\sum \text{INP during SDEs} \pm \text{LOD}}{\sum \text{total INP} \pm \text{LOD}} = \frac{90938 \pm 90.4\ \text{INP}}{121691 \pm 265.1\ \text{INP}} = 74.7 \pm 0.2\% \quad (Eq.3)$$

Dust INP contribution during non-SEDs (23.0%±0.1%)

Dust INP concentration per unit mass of dust aerosols:

$$\frac{\sum \text{INP during SDEs} \pm \text{LOD}}{\sum \text{total INP} \pm \text{LOD}} / \frac{\sum dust_{CAMS} \text{ during SDEs}}{\sum \text{total } dust_{CAMS}} = 97.6\% \quad (Eq.4)$$

$$97.6\% * \left(1 - \frac{\sum dust_{CAMS} \text{ during SDEs}}{\sum \text{total } dust_{CAMS}}\right) = 23.0 \pm 0.1\% \quad (Eq.5)$$

In total, 97.5 ± 0.3% of INPs are from dust particles

4.3 Backtracking SDEs with the European ceilometer network

- **The observed relation: INPs vs. ceilometer signals**

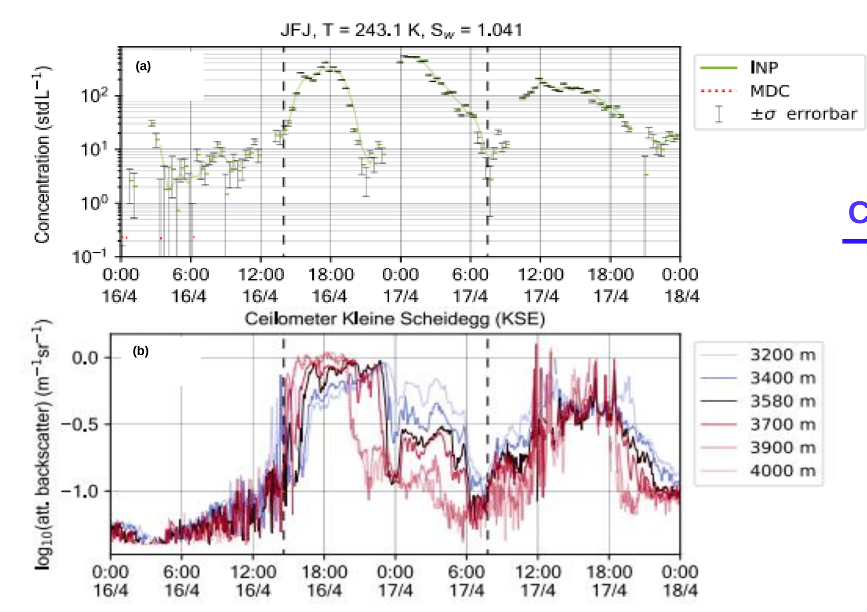

Figure 6. (a) INP concentrations and (b) ceilometer signal at selected altitudes similar to the altitude of the JFJ with filtering for signals in cloud and in precipitation during a classified dust event (April 16-April 17)

Correlation

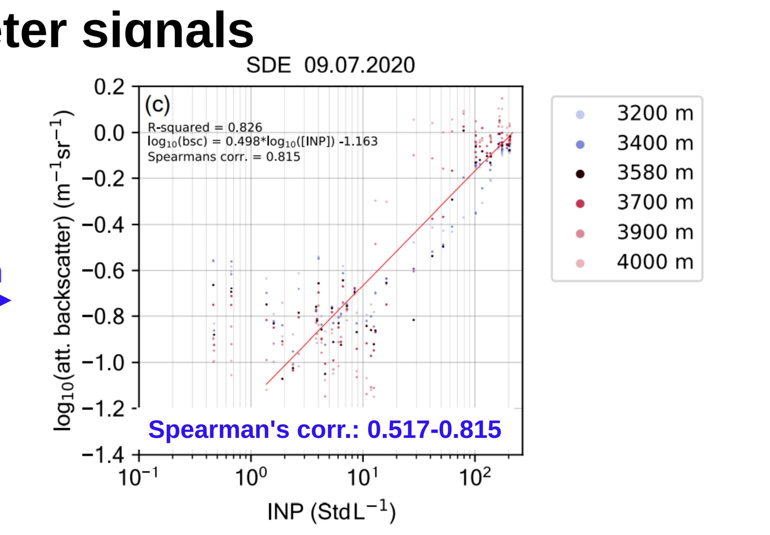

Figure 7. Scatter plots of simultaneous INP concentrations and attenuated backscatter signal at the KSE for a on July 09, 2020.

$$INP_{243K}conc. = 10^{2.062\log_{10}(ABSc)+2.81}$$

INPs: at 243 K, S_w=1.04; ABSc-attenuated back scatter by ceilometer

5 Summary and Outlook

- Sahara dust increase the INP concentrations in the atmosphere of JFJ. Combined with the INP results and the satellite retrieved analysis from CAMS, we propose that 97.5±0.3% of all INPs are from dust particles.

- The attenuated backscatter signal from ceilometers can be used to study atmospheric pathway and temporal evolution of INPs in dust plumes. The resulting correlation should be further validated at other locations where ceilometer data are available.